RSC Advances

ROYAL SOCIETY OF CHEMISTRY

www.rsc.org/advances

Studies on the Langmuir-Blodgett films of Polythiophene containing mesogenic side chain

Chandrasekaran Suryanarayanan[a$], Kamatchi Sankaranarayanan, [b1] Chinthalapuri Divakara[a] , Narayanasastri Somanathan* [a+]

[a] Polymer laboratory, [b]Chemical laboratory, +CSIR-Network of Institutes for Solar Energy, India and CSIR-Central Leather Research Institute. Adyar, Chennai 600 020, India

Present address

[1]Dr. Kamatchi Sankaranarayanan

DST-INSPIRE Faculty,

Centre for Energy and Environmental Science and Technology

National Institute of Technology,

Tiruchirappalli 620 015, Tamil Nadu, India

[$]School of Engineering and Sciences,

Jacobs university, 28719 Bremen, Germany.

Corresponding Author *E-mail: nsomanathan@rediffmail.com

Tel. 0091-44-24437189

FAX 0091-44-24911589

Key words: LB films- polythiophene-absorption-photoluminescence-FTIR

Abstract

Polythiophene containing hexyloxy (PTC6) and tetradecyloxy (PTC14) mesogenic side chains were synthesized. Langmuir films of these polymers at air/water interface were characterized using surface pressure – area (π-A) isotherms and hysteresis from compression - expansion cycle using two spreading solvents $CHCl_3$ and CH_2Cl_2. Langmuir - Blodgett films (LB films) of these polymers were transferred to quartz, silicon and ITO substrates and were analyzed using polarized UV-Vis, Fluorescence. The orientation of the different functional groups in the LB films was compared with spin coated films using polarized FTIR. The studies show that LB films of PTC6 in CH_2Cl_2 show high dichroic ratio suggesting high orientation. Atomic force microscopy (AFM) study reveals the high particulate size morphology in LB films of PTC6. The results from the studies show that solvation and the length of the non-chromophoric alkoxy side chain control the formation of thin films, order and the optical properties of the films.

Introduction

Polythiophenes are π-conjugated polymers having wide applications in photo diodes, sensors and solar cells due to the delocalization of the π-electrons in the main chain.[1] Polythiophene and its derivatives in particular have been the subject of many recent studies due to their environmental stability, high electrical conductivity.[2,3] Several thiophene derivatives containing different heteroatom linkers have been used as potential candidates for solid state polymerization.[4] It has been shown recently that mixtures of terthiophene and bithiophene can be tailored to suit the needs of optical devices such as solar cells, sensors and organic light emitting diodes.[5]

Thiophene based molecules are an elegant example of organic materials with superior transport properties having the advantage of planar and highly conjugated backbones. These systems can form orderly packed arrangement in thin films with a strong π-π interchain interaction, which enhances charge-transport. In a recent study, 2D π-conjugation of alkyl-dithiophene side chains is shown to promote red shifted absorption profiles, low HOMO energy levels (<−5.6 eV) and enhanced environmental and thermal stability.[6]

However, fabrication of these synthetic polymers to control the molecular architecture for optimized physical properties is a crucial step in the final product output. Langmuir- Blodgett (LB) technique is an important tool to prepare ordered ultra-thin films of amphiphilic materials. It has several advantages over other methods which are based on chemical or physical deposition techniques, for achieving a highly organized molecular arrangement.[7-10] Methods other than LB technique are reported to give a wide variation in the electrical and optical characteristics of field effect transistors, light emitting diodes and solar cell.[11-13] LB technique allows precise control of the monolayer thickness, homogeneous deposition of the monolayer over large areas and the possibility to make multilayer structures with varying layer composition, and can be deposited on any kind of solid substrate.

In all these cases, it is desirable to synthesize a molecule, which can be tailored to get optimal film thickness for simulated end use application. It has been shown that poly (3-alkyl thiophene)[14,15] in which the alkyl chains placed along the polymer side chain lead to reduced

charge carrier mobility due to steric hindrance. LB films of polythiophene onto step-bunched Si substrate has been proved to be effective for controlling the in-plane molecular arrangement.[16] Here, attempts have been made to achieve highly organized arrangement of the molecules by using a water soluble amphiphile like 1-dodecanol as a molecular lubricant. Even though dodecanol succeeds in preventing premature aggregation, there is a decrease in charge carrier mobility due to pinhole formation in thin film. Long chain fatty acids have been added to form a supporting matrix, but this results in additional complications like stability of fatty acid over a period of time, and the structural ordering of the molecule that reduces the device performance.[17] Tanese et al. has reported Langmuir-Schäfer technique for regio regular Poly(2, 5-dioctyloxy-1, 4-phenylene-*alt*-2, 5-thienylene) in which the back bone planarity has been improved.[18] An effort has also been made to overcome the structural ordering by changing the molecular back bone of thiophene to achieve the desired electrical and optical properties. The substitution of tetra hydro pyranyl functional group results in large scale molecular level ordering[19] with preferential alignment of main chain along the transfer direction of thin films. The change in end group with carboxylic acid and alkane with change in solvents (THF/$CHCl_3$) resulted in inversion of the structural segments in the thin films at air/ water interface.[20] Azizian *et al* has reported the surface phase transition studies using IR at the Air/Water Interface.[21] Collins et al. have reported the photo elastic modulated FTIR on films at air/water interface.[22] The influence of linking group on the surface isotherm and packing is reported.[23]

In the present study, Langmuir films of Poly4-{(E)-[(4-alkoxy phenyl imino]methyl}phenyl thiophene-3-carboxylate (Fig. 1) have been studied. The influence of alkoxy chain length and spreading solvents like dichloromethane (CH_2Cl_2), chloroform ($CHCl_3$) on the film properties of Langmuir Blodgett films of Poly 4-{(E)-[(4-hexyloxy phenyl imino]methyl}phenylthiophene-3-carboxylate (PTC6) and Poly4-{(E)-[(4-tetradecyloxy phenyl imino]methyl}phenylthiophene-3-carboxylate (PTC14) has been carried out. The orientation of the LB films calculated using order parameter was compared with spin coated thin films, usually used under simulated end use conditions in diodes. The morphology of LB films of PTC6 and PTC14 in different solvents on different substrates was studied using atomic force microscopy (AFM).

Experimental methods

The detailed synthetic procedure of the monomers and polymers was presented in our earlier publication[24,25] and the details of PTC6 and PTC14 and polymerization and structural confirmation using NMR, ESI-MS and Elemental analysis is given in supporting information. (Mn=7475,Mw=20780 and PDI=2.78)[24]; Regioregularity of PTC6- 57.89%; PTC14- 61.11% calculated from proton NMR[26]. Langmuir films of the thiophenes in HPLC grade dichloromethane and chloroform purchased from Merck (99.9% pure) was used for all experiments. The sub-phase was prepared with millipore milli-Q deionized water (Millipore, resistivity greater than 18.2 Ω). 0.1 mg/ml of each sample was taken for the preparation of Langmuir films at the air/water interface. The Langmuir-Blodgett films (LB films) of these were transferred onto solid substrates which were earlier cleaned with freshly prepared chromic acid, washed with deionized water and stored in desiccators. 10 µl of the solutions were carefully spread onto the surface of the clean water sub phase, drop wise using a Hamilton syringe. After the solvent had evaporated completely (~20 min), the molecules at the air/water interface were compressed at a barrier speed of 20 or 50 mm/min. A Langmuir minitrough (NIMA mini PS4, U.K.) was employed for the preparation of the films. The interface was thoroughly cleaned by compressing the barriers to ensure that the maximum surface-pressure difference was less than 0.2 $mN \cdot m^{-1}$ upon compression. Chloroform and dichloromethane were used as spreading solvents to prepare the Langmuir films of PTC6 and PTC14 and the surface-pressure−area (π−A) isotherm was recorded.

LB films with odd number of layers of polymers were deposited from the air/water interface by vertical dipping onto freshly cleaned quartz substrates (10 × 10 mm), transparent indium−tin oxide (ITO) glass substrates (10 × 10 mm^2, R_s = 100 Ω/square, Sigma Aldrich) . The LB deposition was carried out at a dipping rate of ~ 10 mm/min under a constant surface pressure of about 15 mN/m.

Linear dichroism for the LB films was carried out using Cary Bio-50 spectrophotometer. A prism polarizer placed in the path of the incident light is mounted on a graduated rotating base

that could be dialed to generate plane-polarized light at various angles relative to the substrate of the sample. Polarized absorption spectra have been taken at angles of 0° (horizontal-H) and 90° (vertical-V). An order parameter from Linear Dichroic (LD) measurement of the films has been used to analyze the orientation. Here R- the ratio between absorbance for p and s-polarized light LD- is used to calculate the order parameter which is defined as

$$\text{Order parameter} = (R-1)/(R+2) \quad (1)$$

The polarized absorption spectra have been corrected for scattering by using a simple algorithm that removed scattering so that the correction satisfied two criteria. First, the scattering correction had to satisfy the simple formula $a+b\lambda^{4}$, where 'a' and 'b' are independent variables. We made the further assumption that the scattering correction is identical (isotropic) for both polarization angles. This prevents the scattering correction from having an influence on the calculation of the transition dipole.

Photoluminescence (PL) polarization experiment for LB films was recorded by using Cary Eclipse fluorescence spectrometer. The polarizer and analyzer were placed beside the LB film (over quartz substrate) and the spectrum was recorded by varying the position of the polarizer and analyzer (Horizontal (H) and Vertical (V) position). The fluorimeter is not corrected for the wavelength dependence of the sensitivity of the detection channel

AFM analysis for LB films transferred over ITO substrate was done using Nova 1.0.26 RC1 with NT-MDT solver software for analysis. Silicon cantilever (SII) with average frequency of 260-630 kHz with force constant of 28-91 N m^{-1}were used in semi contact mode.

FT-IR measurements were performed on MB 3000 spectrometer at a resolution of 4 cm^{-1}, and 32 scans were accumulated. Polarized FT-IR spectra were obtained by using a ZnSe wire grid polarizer (PIKE technologies) positioned before the specimen. The infrared beam was polarized parallel or perpendicular to that of the specimen. The position of the specimen was kept at Brewster angle constant throughout the measurement.

Results and discussion

Surface Pressure–area isotherm of PTC6 and PTC14

Since choice of solvent, rate of drying, thermal annealing and vapour annealing is shown to affect the photovoltaic device performance,[27] surface pressure-area (π - A) isotherms were obtained for PTC6 and PTC14 with two different spreading solvents (CH_2Cl_2 and $CHCl_3$) and at two different compression speed (20 and 50 mm/min) and presented in Figure 2. For all the experiments, the concentration and other conditions (as mentioned earlier) were kept constant for all the polymers. The isotherm shows steady rise in surface pressure with decrease in the monolayer area and the relative collapse pressure is listed in Table 1. The two polymers on compression showed a liquid expanded state (LE) with average area varying between 4 nm^2 (PTC6) and 5 nm^2 (PTC14). The results show that films formed using CH_2Cl_2 have lower area compared to the films spread using $CHCl_3$ at the air/water interface. The different pressure-area isotherms found for CH_2Cl_2 and $CHCl_3$ are perhaps due to a better solubility of the polymer in $CHCl_3$.This is may also be indicative of planarization of the conjugated backbone together and change in packing of the both PTC6 and PTC14 in the presence of CH_2Cl_2.

As control experiment, we had carried out experiments of the precursor material (before attaching the fatty chain) as Langmuir films and this did not show any surface pressure. So the surface pressure seen in the π-A graph should be mainly due to the amphiphilic nature of the compound. The large surface area per repeat unit is mainly because of the bulky head group containing thiophene together with the shorter side chain organizing at the air/water interface. Such large surface area per repeat unit for derivatives of poly(ethylene oxide) have been studied [28]. Our earlier studies[25] on the hetero correlation analysis of variable temperature XRD and variable temperature IR studies of the above polymers show that the packing is influenced by the alkoxy chain length and planarization takes place in the organisation.

The compression modulus C_s^{-1} is a parameter used to define the different states of the monolayer and the collapse pressure and is obtained from the equation.

$$C_s^{-1} = -A\,(\partial\pi/\partial A) \quad (2)$$

Generally its values lower than 12.5 mN/m are attributed to the gaseous state, values between 12.5 and 100 mN/m to the liquid expanded state, and 100 to 250 mN/m to the liquid condensed state, while C_s values greater than 250 mN/m are assigned to the solid state of the film. At the collapse pressure the value approaches zero.[29]

Using this criterion, the maximum collapse pressures for the different systems used in the present study have been estimated. Table 1 shows the maximum collapse pressure of different monolayers prepared with different solvents. The low collapse pressure of PTC6 together with low compression modulus indicates that the entrainment of CH_2Cl_2 in the film may make it incompressible for the given area. This trend is also seen for PTC14 suggesting that CH_2Cl_2 may not be a suitable solvent to prepare homogeneous densely packed films.

Figure 3a and b shows the representative hysteresis cycle of the PTC6 on repeated compression and expansion of the monolayer at the air /water interface prepared with $CHCl_3$ and CH_2Cl_2 respectively. In order to assess the stability of these films at air/water interface, all the films were maintained at a constant pressure below that of the collapse pressure. In Fig (3a) there is a significant reduction in area for PTC6 with $CHCl_3$ spread monolayer. The compression modulus and the large area that are seen in Fig 2(a), Fig 2(b) for $CHCl_3$ spread films show clearly that local organisation at the interface can be easily redistributed, and this is in agreement with hysteresis plot. With CH_2Cl_2 as spreading solvent, (Fig (3b)) the area remains the same indicating the non-elastic behaviour of the film.

The hysteresis ratio calculated by taking the ratio of the energy lost during hysteresis to the total energy applied for the onward cycle (supp info) indicates that, films of PTC6 prepared using CH_2Cl_2 show no characteristic variation in hysteresis ratio for first compression, while the same film shows a further decrease in hysteresis ratio during second cycling. For films prepared with $CHCl_3$, the first cycle shows plastic nature, which stabilizes on further cycling, enhancing the elastic nature of the film.

The stability of the Langmuir films has been tested using the hysteresis analysis well below the collapse pressure of the film, where the transfer to solid surfaces was done.

The rate of change of area ($\Delta A/A$) per unit time from the hysteresis analysis is given below:

For PTC6 in CH_2Cl_2 it is 0.9 and 0.59 respectively for first and second cycle, while in $CHCl_3$ the obtained values are 0.97 and 0.77 respectively for first and second cycle. The obtained values for PTC14 in CH_2Cl_2 , the obtained values are 0.85 and 0.6 respectively for the first and second cycle; while the values obtained in $CHCl_3$ are 0.89 and 0.77 respectively for first and second cycle. The rate of change of area for a neat film on compression and expansion should be same. However, any hysteresis curve is expected to have lost some amount of film material based on the property of the material. The material is stable as Langmuir films

Polarised FTIR studies

Polarised infrared spectroscopy can be used to provide information about the direction of transition dipole moments of the normal modes of vibrations. The FTIR spectra of LB films transferred to silicon wafers is presented in Figure 4 for 2800 - 3000 cm^{-1} region where the variation is characteristic. The wave numbers of vibrations corresponding to different functional groups obtained for different vibrational modes is presented in Table 2. On an average, there is a shift of about 3 to 7 cm^{-1} change between the frequencies of stretching for films formed from CH_2Cl_2 and $CHCl_3$. However, for C=O the change is of the order of 12 to 15 $cm^{-1.}$ The main chain also shows a characteristic change due to the influence of solvents and the δ_{C-H} of thiophene of PTC6 is shifted from 813 to 817 cm^{-1} [30] (for CH_2Cl_2 films compared with $CHCl_3$ films). Comparison of the IR peaks of the LB films of PTC6 and PTC14 shows that the alkoxy chain length influences the stretching vibration of the alkyl chains and there is a 7 cm^{-1} shift in asymmetric stretching (ν_{as}) on going from PTC6 to PTC14. The influence of inductive effect of alkoxy chain is also felt by the C=O stretching and for the same CH_2Cl_2 solvent there is a 15 cm^{-1} (1748-1733 cm^{-1}) shift.

Spin coated films prepared from the two solvents also showed similar trends. The ν_{as} CH_2 of PTC6 shows a 4 cm^{-1} change for CH_2Cl_2 to $CHCl_3$, while the symmetric stretching is much more influenced by the solvents for PTC6. It is interesting to note that in the case of PTC14, a reversal trend is seen for ν_{as} CH_2 (Table 2). Due to the influence of inductive effect and solvation ν_{as} C=O is more red shifted.

On comparing LB films and Spin coated films there is a red shift in alkyl region stretching vibrations. The effect is also more pronounced in the C=O region in LB films compared to spin coated films. The influence of solvents and alkoxy chain length on orientation of the polymers is understood by comparing the dichroic ratio (DR) and presented in Table 2. DR values close to 1 means there is no preferred orientation and the film may be tending to disorder. The values >>1 indicate better order. The alkyl groups present in LB films are ordered and are influenced by the solvent. In PTC6, CH_2Cl_2 influences strongly and controls the orientation of alkyl groups, whereas $CHCl_3$ brings in marginal effect. The above is also seen in ν_s C-O-C and the groups corresponding to main chain, which can be attributed to the hindered rotation of the phenoxy unit, and the DR is 5.95 for CH_2Cl_2 based LB film.[31] Similar trend is seen for LB films of PTC14, but the degree of variation is less when compared to PTC6.

The trend followed in LB films is seen in spin coated films too. PTC6 and PTC14 thin films prepared using CH_2Cl_2 show higher variation at all vibrational modes compared to $CHCl_3$. The effect is much pronounced in vibrational modes corresponding to alkyl regions. Due to the influence of aggregation, solvation and the inductive effect produced by the alkyl chain, the disorder is high in spin coated films when compared to the packing of LB films. CH_2Cl_2 brings in order in both LB films and spin coated films of PTC6 and PTC14 when compared to $CHCl_3$.

Polarised UV and Photoluminescence studies

Since the materials are highly photoactive, the absorption spectra of the LB films transferred over quartz and those of the spin coated films were recorded. The characteristic peaks (by deconvalution of the spectra) obtained for LB films and spin coated films are compared in Table 3 and the obtained absorption spectra for solution, LB films and spin coated films of PTC6 and PTC14 are presented in Fig. 5. Solution spectra of PTC6 and PTC14 in various solvents were compared in Table 3. The absorption spectra in solution clearly show besides the maximum in the range 300-400nm (which is probably due to the side chains) a second band in the range 500-600 nm which corresponds better with what is observed for polythiophene. Comparison of the absorption wavelengths obtained for LB films with the solution data show that all absorption wavelengths shift to lower wavelength in LB film. Table 3 indicates that the solvent used for the preparation of films influence the packing and therefore the λ_{max} of the thin films varies. When

compared with LB films there is red shift in solution and the red shift is higher in the case of PTC14 when compared to PTC6 indicating that the alkoxy chain length modifies orientation of packing. In a first approximation, from the dipole interaction between chromophore in the linear aggregate, it is expected that the absorption band due to the transition moment that lays flat exhibits a red shift, while that standing vertically exhibits a blue shift.[32]

The change in orientational order parameter was calculated using linear dichroism and the values obtained for LB films for different solvents is computed in Table 4. The order parameter is high in PTC6 $CHCl_3$ based films. Whereas the value is higher in PTC14 films prepared using CH_2Cl_2. In general, PTC14 is more influenced by the solvents on packing. Comparison of the order parameter (Table 4) obtained for PTC6 and PTC14 indicate the order is more pronounced in PTC6. Similar to infrared spectra, aggregation, solvation, rate of withdrawal of solvent from different groups during film formation and the influence of alkoxy chain length, influence the orientational order parameter of spin coated films, but the order is less when compared to LB films.

The photoluminescence spectra obtained for LB and spin coated films with the polariser position 'HH' and 'VV' are presented in Figure 6. The photoluminescence emission spectra of both polymers show all three base colour emissions, apart from emission in UV region. In the case of PTC6 there is a red shift of about 11 nm (353 to 364) on changing solvent from $CHCl_3$ to CH_2Cl_2, while in PTC14 it's only 5 nm (367 to 372). The above result validates not only the effect of solvent but also the inherent structural organisation of the polymer with change in non chromophoric alkoxy chain length. The detailed analysis on all three base colours of polymers show that blue centred emission for the LB films of both polymers prepared with $CHCl_3$ shows high intensity. The dichroic ratio (supplementary information) is obtained from the ratio of the PL intensity at 'HH' to 'VV' position of the polariser. The intensity at 'HH' position is always lower than the intensity 'VV' suggesting that there is preferential orientation. The dichroic ratio observed in the UV region is high compared to the other colour regions of the spectrum. The results obtained from the experiments (table in Supp info) suggest that the green emission is highly polarised than the other regions. Both LB and Spin coated films prepared with $CHCl_3$

show lower dichroic ratio value when compared to films prepared with CH_2Cl_2. This suggests that the chromophore are more scattered on the surface of the films.

AFM Morphology Studies

The AFM images of LB films are presented in Figure 7(a - d). The LB films of PTC6 prepared from CH_2Cl_2 (Fig 7b) orients in the transfer direction and show morphology of uniform grid like pattern with crests and troughs. Line profile analysis (Figure 7a & 7b) of PTC6 $CHCl_3$ and CH_2Cl_2 reveals uniform grids of approximately 2.1 μm width. For PTC6 in CH_2Cl_2 LB film with increase in agglomerate intensity of about 12 nm compared to PTC6 $CHCl_3$ LB film. In the case of PTC6 $CHCl_3$ film, the particulate size is big and forms uniform surface and its line profile analysis shows uniform profile height with random undulation in μm domain. Due to this, it is expected that the intensity of PL will be higher in the films of PTC6 from $CHCl_3$.[27] It is interesting to note that the AFM images of PTC14 LB films from CH_2Cl_2 (Fig. 7d) organise into a higher domain arranged in the direction perpendicular to the dipping / transfer direction with higher intensity of about 300 nm. The agglomerates present on the surface also show a preferred angular orientation in the LB films of PTC14 from CH_2Cl_2. LB films of PTC14 ($CHCl_3$) (Fig 7c) shows high roughness, when compared to the LB films with CH_2Cl_2 due to the decrease in particulate intensity with random distribution on the surface.

The working of devices (solar cell and OLEDs) involves coulombically bound electron-hole pairs; thus, an adequate driving force for charge separation must exist for full separation of electron and hole pairs; for this adequate device architecture must exist for excitons to diffuse through the donor-acceptor interface for efficient device function.[33] LB is one of most advantageous method to control morphology and film thickness for organic electronics.[34] The PTC6 and PTC14 show change in molecular assembly, which can change the final device output. A schematic representation of the possible organisation of polymers over air/water interface is presented in Figure 8, in which the π conjugated backbone attached to nonpolar functional group is located above the thiophene head polar group. The change in solvent polarity can lead to disparity among polar functional groups in π-conjugated backbone on increasing solvent polarity from $CHCl_3$ to CH_2Cl_2.

From the intricate analysis of Polarised FT-IR and AFM measurement of transferred LB film, it is found that the domain structure varies with the alignment of functional groups present in the side chain. As shows in Fig 8b, the change in solvent polarity may have greater influence over torisonal angle of main body functional groups, so change in polarity invariably varies the torisonal angle between the thiophene main chain and C=O and azomethine which brings in aggregation of main body with change in tail alkyl groups. Piliego et al. reported that in π-conjugated polymer backbone, crystallinity varies with change in solvent polarity with change in charge carrier mobility.[35] Such changes in film thickness is associated with a more complete coverage of adsorption sites in thicker films due to diffusion of polymer polar functional groups present in it.[36] Dichloromethane on evaporation should have brought more interaction among polar functional groups than chloroform resulting in clubbing of alkyl chain which may results in grid pattern in AFM images and higher dichroic ratio in Polarised IR studies for CH_2 alkyl chain.

Conclusion

Control of morphology at the microscopic scale is critical for optimizing the device efficiency in organic opto-electronics. The results show that films prepared with CH_2Cl_2 are better ordered than those prepared with $CHCl_3$. The increase in alkoxy chain length in the LB film leads to a more viscoplastic and flexible film. In spin coated films, the aggregation, solvation and the rate of withdrawal of solvent from different functional groups during the spin coated film formation and the influence of alkoxy chain length, results in the lower orderliness in spin coated films compared to LB films. IR experiment shows CH_2 ν_{sym} stretching vibration lower absorption for CH_2Cl_2 as spreading solvent indicates bonding interaction between alkyl chains. This view is supported by the red shift in UV on changing solvent from $CHCl_3$ to CH_2Cl_2 and the AFM supports the control of morphology with the solvent polarity used for preparation.

Acknowledgment

The authors thank Dr. A. Ajayaghosh and Mr. R. Thirumalai, CSIR-NIIST, Trivandrum for their help in AFM studies. The authors gratefully acknowledge financial support from the Council of Scientific and Industrial Research (CSIR), Network project NWP55.

References

1 T. Yamamoto, *NPG Asia Mater.* 2010, **2**, 54.

2 A. Laforgue, P. Simon, C. Sarrazin and J.F. Fauvarque, *J. Power Sources* 1999, **80**, 142.

3 M. Mastragostino, C. Arbizzani and F. Sovai, *J. Power Sources* 2001, **97**, 812.

4 C. Tusy, L. Huang, J. Jin and J. Xia *RSC Adv.,* 2014, **4**, 8011.

5 B. Kolodziejczyk, D. Mayevsky and B. Winther-Jensen *RSC Adv.,* 2013, **3**, 4568.

6 M. Bolognesi, D. Gedefaw, D. Dang, P. Henriksson, W. Zhuang, M. Tessarolo, E. Wang, M. Muccini, M. Serid and M. R. Andersson *RSC Adv.,* 2013, **3**, 24543.

7 H.E. Katz, Z. Bao and S.L. Gilat, *Acc. Chem. Res.* 2001, **34**, 359.

8 X. Chen, B. Liu, H. Zhang, S. Guan, J. Zhang, W. Zhang, Q.Chen, Z. Jiang and D. Guiver, *Langmuir* 2009, **25**, 10444.

9 R.B. Pernites, M.J. Felipe, E.L. Foster and R.C. Advincula, *Appl. Mater. Interfaces* 2011, **3**, 817.

10 X. Feng, V. Marcon, W. Pisula, M.R. Hansen, J. Kirkpatrick**,** F. Grozema, D. Andrienko, K. Kremer and K. Müllen, *Nature Mater.* 2009, **8**, 421.

11 D. Sparrowe, G. Latini, M.Bird, N. Stingelin, *Organic Electronics* 2012, **13**, 173.

12 Z. Luo, H. Shi, H. Zhu , G. Song and Y. Liu, *Dyes and Pigments* 2012, **92**, 596.

13 S.K. Swathi, K. Ranjith, P. Kumar and P.C. Ramamurthy, *Solar Energy Materials and Solar Cells* 2012, **96**, 101.

14 C.V. Hoven, H. Wang, M. Elbing, L. Garner, D. Winkelhaus and G.C. Bazan, *Nature Mater.* 2010, **9**, 249.

15 J. Matsui, S. Yoshida, T. Mikayama, A. Aoki and T. Miyashita, *Langmuir* 2005, **21**, 5343.

16 R. Onoki, G. Yoshikawa, Y. Tsuruma, S. Ikeda, K. Saiki and K. Ueno, *Langmuir*, 2008, **24**, 11605.

17 G. Xu, Z. Bao and J.T. Groves, *Langmuir* 2000, **16**, 1834-1841**.**

18 M.C. Tanese, G.M. Farinola, L. Valli, L. Giotta, S. Conoci, P. Lang, D. Colangiuli, F. Babudri, F. Naso, L. Sabbatini, P.G. Zambonin and L. Torsi, *Chem. Mater.* 2006, **18**, 778.

19 J.S. Mattu and G.W. Leach, *J. Am. Chem. Soc.* 2010, **132**, 3204.

20 J. Chen, A.R. Murphy, J. Esteve, D.F. Ogletree, M. Salmeron and J.M.J. Frechet, *Langmuir* 2004, **20**, 7703.

21 S. Azizian, K. Shibata, T. Matsuda, T. Takiue, H. Matsubara, M. Aratono, *J. Phys. Chem. B*, 2006, **110**, 17034.

22 S.J. Collins, A. Dhathathreyan, T. Ramasami and H. Möhwald, *Thin solid films* 2000, **358**, 229.

23 N. Somanathan, C.K. Pandiyarajan, W.A. Goedel and W.C. Chen, *J. Polym Sci Part B: Polym Phys.* 2009, **47**, 173.

24. C. Suryanarayanan, E. Ravindran, S. J. Ananthakrishnan, N. Somanathan and A.B. Mandal, *J.Mater. Chem*. 2012, **22**, 18975.

25 C. Suryanarayanan, A. Prasannan,, Po-Da Hong, B. Sambathkumar and N. Somanathan, *Mater. Chem. Phy*., 2014, **143** 1352.

26 F.A. Bovey and P.A. Mirau, *"NMR of polymers"* Academic press, SanDiego, 1996 P. 169.

27 M. Campoy-quiles, T. Ferenczi1, T. Agostinelli, P.G. Etchegoin, Y. Kim, T.D. Anthopoulos, P.N. Stavrinou, D.D.C. Bradley and J. Nelson, *Nature Mater*. 2008, **7**, 158**.**

28 A.L. Meader and D.W. Criddle, J. Colloid Sci., 1953, **8**, 170.

29 J.T. Davies, E.K. Rideal, *Interfacial Phenomena,* 2nd ed., Academic Press, NY, 1963.

30 M.S.A. Abdou and S. Holdcroft, *Macromolecules* 1993, **26**, 2954.

31 J.G. Zhao, T. Yoshihara, H.W.Siesler and Y.Ozaki, *Phys. Rev. E* 2001, **64**, 031704.

32 K. Fukuda and H. Nakahara, *J. Colloid Interface Sci.* 1984, **98**, 555.

33 B. Carsten, J.M. Szarko, H.J. Son, W. Wang, L. Lu, F. He, B.S. Rolczynski, S. J. Lou, L.X. Chen and L. Yu, *J. Am. Chem. Soc.* 2011, **133**, 20468.

34 A. Ulman, An Introduction to Ultra-thin Organic Films from Langmuir–Blodgett to Self-assembly, Academic Press, London, 1991.

35 C. Piliego, T.W. Holcombe, J.D. Douglas, C.H. Woo, P.M.Beaujuge and J.M.J. Frechet, *J. Am. Chem. Soc*. 2010, **132**, 7595.

36 N.C. DeSouza, V. Zucolotto, J.R. Silva, F.R. Santos, D.S. DosSantos, D.T. Balogh, O.N. Oliveira and J.A. Giacometti, *J. Colloid Interface Sci.* 2005, **285**, 544.

Table 1. Maximum collapse pressure and compressibility modulus for all polymers with two different solvents (CH_2Cl_2 / $CHCl_3$) and at two different compression rates (20/50) mm/ min.

Spreading solvent	Sample name (Barrier speed mm/min)	Collapse pressure (mN/m)	Compression Modulus (C_s^{-1}) (mN/m)
$CHCl_3$	PTC6 (20)	8.54	0.199
	PTC6 (50)	12.12	0.076
	PTC14 (20)	21.57	0.252
	PTC14 (50)	20.76	0.334
CH_2Cl_2	PTC6 (20)	9.06	0.111
	PTC6 (50)	8.24	0.160
	PTC14 (20)	14.91	0.372
	PTC14 (50)	15.4	0.539

Table 2. IR Dichroic ratio ($Abs_{\parallel}$ / $Abs_{\perp}$) table for LB and spin coated film and its respective spreading solvents

[a] Symmetric stretching - ν_s ; asymmetric stretching - ν_{as} ; bending vibration - δ

Wave number assignments [a]	LB Film								Spin coated film							
	PTC6				PTC14				PTC6				PTC14			
	CH_2Cl_2		$CHCl_3$		CH_2Cl_2		$CHCl_3$		CH_2Cl_2		$CHCl_3$		CH_2Cl_2		$CHCl_3$	
	ν (cm^{-1})	DR	ν (cm^{-1})	DR	ν (cm^{-1})	DR	ν (cm^{-1})	DR	ν (cm^{-1})	DR	ν (cm^{-1})	DR	ν (cm^{-1})	DR	ν (cm^{-1}	DR
ν_{as} CH_3	2954	28.9	2951	1.06	2956	0.77	2956	-0.89	2953	1.27	2955	0.96	2958	0.62	2956	0.97
ν_s CH_3	2873	39.89	2868	1.01	2872	0.25	2875	-0.86	2873	1.26	2871	0.92	2873	0.62	2870	0.98
ν_{as} CH_2	2920	21.07	2918	1.02	2927	0.25	2925	-0.85	2916	1.25	2920	1.02	2920	0.63	2916	0.98
ν_s CH_2	2852	28.01	2854	0.98	2852	-4.81	2856	-0.87	2848	1.12	2854	1.71	2849	1.04	2849	0.95
ν_s C=O	1748	-1.46	1739	1.09	1733	-21.74	1726	-0.83	1737	1.22	1734	0.72	1735	0.51	1733	1.17
ν_s C=C	1506	-1.38	1507	1.75	1508	0.87	1506	0.65	1507	1.12	1508	1.09	1506	0.30	1508	0.91
ν_s C-O-C	1107	5.95	1105	1.47	1105	3.68	1106	-0.34	1109	1.65	1108	0.98	1109	0.57	1108	0.93
δ_{C-H} in plane of thiophene.	813	9.71	817	1.93	817	0.93	817	-1.15	816	1.24	811	0.84	817	0.62	818	0.94
δ_{C-H} in plane bending of phenyl.	738	4.88	740	1.71	739	1.39	737	-0.16	736	1.24	735	0.88	738	0.64	739	1.01

Table 3. Photo absorption spectral data of LB films, spin coated films and solution spectra in CH_2Cl_2 / $CHCl_3$ solvents.

Sample Code	Solution UV Wavelength (nm)		LB film UV Wavelength (nm)		Spin coated UV Wavelength (nm)	
	CH_2Cl_2	$CHCl_3$	CH_2Cl_2	$CHCl_3$	CH_2Cl_2	$CHCl_3$
PTC6	255, 333, 355, 450.	254, 335, 469.	236, 291, 333.	233, 284, 336.	238, 261, 353.	231, 262, 353.
PTC14	256, 338, 457.	263, 336, 454.	238, 306, 336.	231, 281, 337.	241, 269, 353.	235, 254, 351.

Table 4. Orientational order parameter calculated using linear dichroism and the values obtained for LB and spin coated films for different solvents.

Sample	UV order parameter	
	LB film	Spin coated film
PTC6 $CHCl_3$	0.46	0.183
PTC6 CH_2Cl_2	0.306	0.12
PTC14 $CHCl_3$	0.021	0.292
PTC14 CH_2Cl_2	0.16	-0.157

Legends for the Figures

Fig 1. 4-{(E)-[(4-alkoxy phenyl)imino]methylphenylthiophene-3-carboxylate

R = -C_6H_{13} (PTC6); -$C_{14}H_{29}$ (PTC14)

Fig 2. The π-A isotherms of (a) PTC6 and (b) PTC14 with two spreading solvents (CH_2Cl_2 / $CHCl_3$) and at two compression rates 20-50 cm/min

Fig 3. Surface pressure–molecular area (π–A) isotherms of PTC6 compression and expansion cycles is shown in arrows and number of cycles is shown in numbers (a) $CHCl_3$ and (b) CH_2Cl_2 as spreading solvents and PTC14 in (c) $CHCl_3$ and (d) CH_2Cl_2 as spreading solvents

Fig 4. FT-IR overlaid spectrum of (a) PTC6 and (b) PTC14 samples in 2800-3000 cm-1 for LB and spin coated film prepared with two different (CH_2Cl_2/$CHCl_3$) solvents

Fig. 5 Absorption spectra of PTC6 and PTC14 (a) solution (b) LB film (C) spin coated film

Fig 6. Photo luminescence spectra of LB coated films of PTC6 (a) and PTC14 (b) in $CHCl_3$ and CH_2Cl_2

Fig 7. The AFM scanned image of PTC6 (a) $CHCl_3$, (b) CH_2Cl_2; PTC14 (c) $CHCl_3$, (d) CH_2Cl_2

Fig 8. Schematic representation of dynamic bond variation organized according to the interaction between components with solvent and two different functionalities

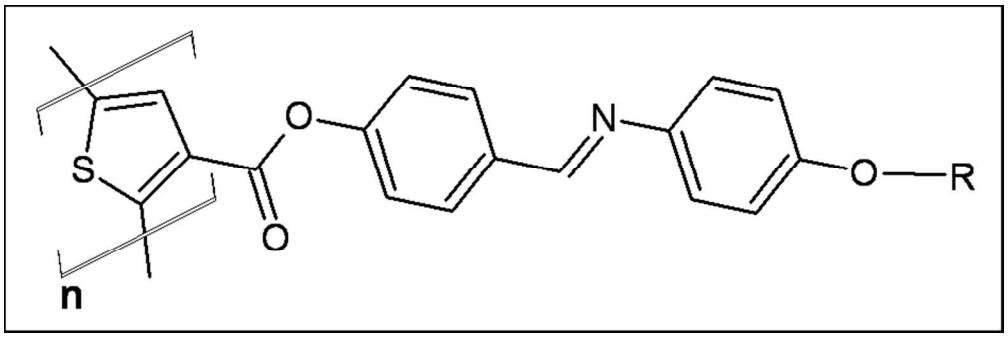

4-{(E)-[(4-alkoxy phenyl)imino]methylphenylthiophene-3-carboxylate
R = -C6H13 (PTC6); -C14H29 (PTC14)

159x52mm (150 x 150 DPI)

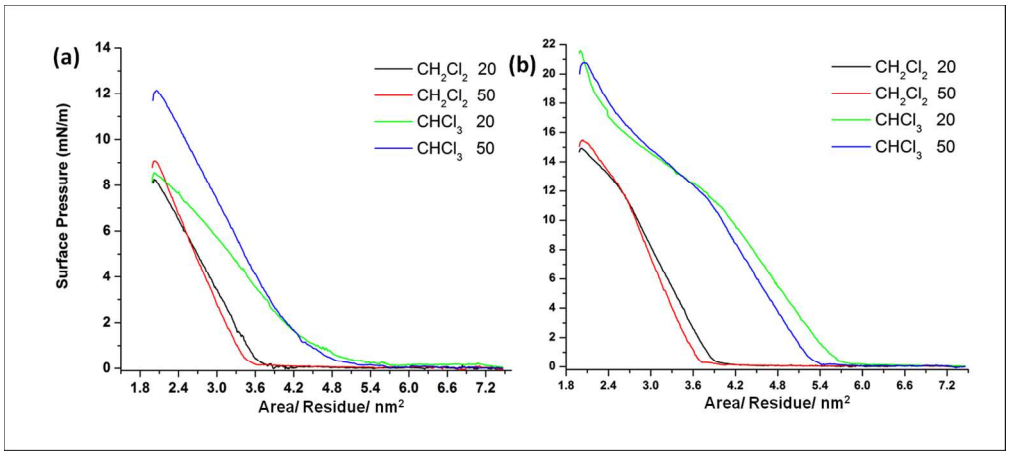

The π-A isotherms of (a) PTC6 and (b) PTC14 with two spreading solvents (CH2Cl2 / CHCl3) and at two compression rates 20-50 cm/min
261x116mm (150 x 150 DPI)

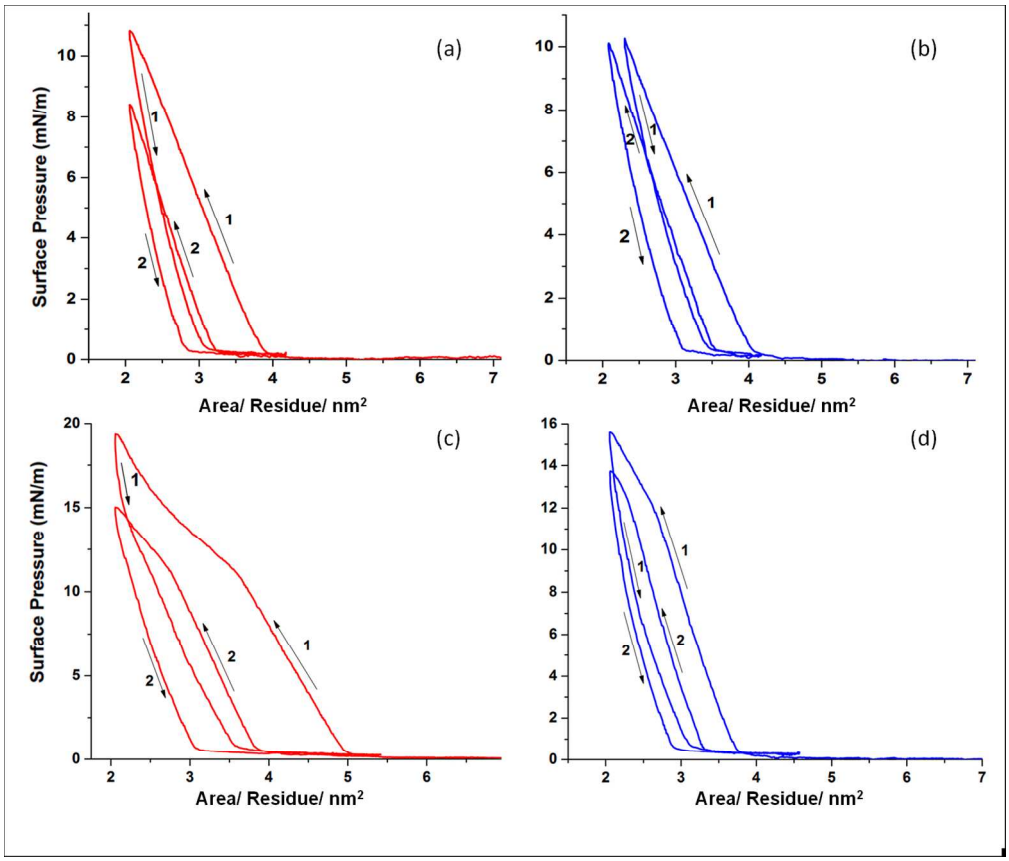

Surface pressure–molecular area (π–A) isotherms of PTC6 compression and expansion cycles is shown in arrows and number of cycles is shown in numbers (a) CHCl3 and (b) CH2Cl2 as spreading solvents and PTC14 in (c) CHCl3 and (d) CH2Cl2 as spreading solvents
266x226mm (150 x 150 DPI)

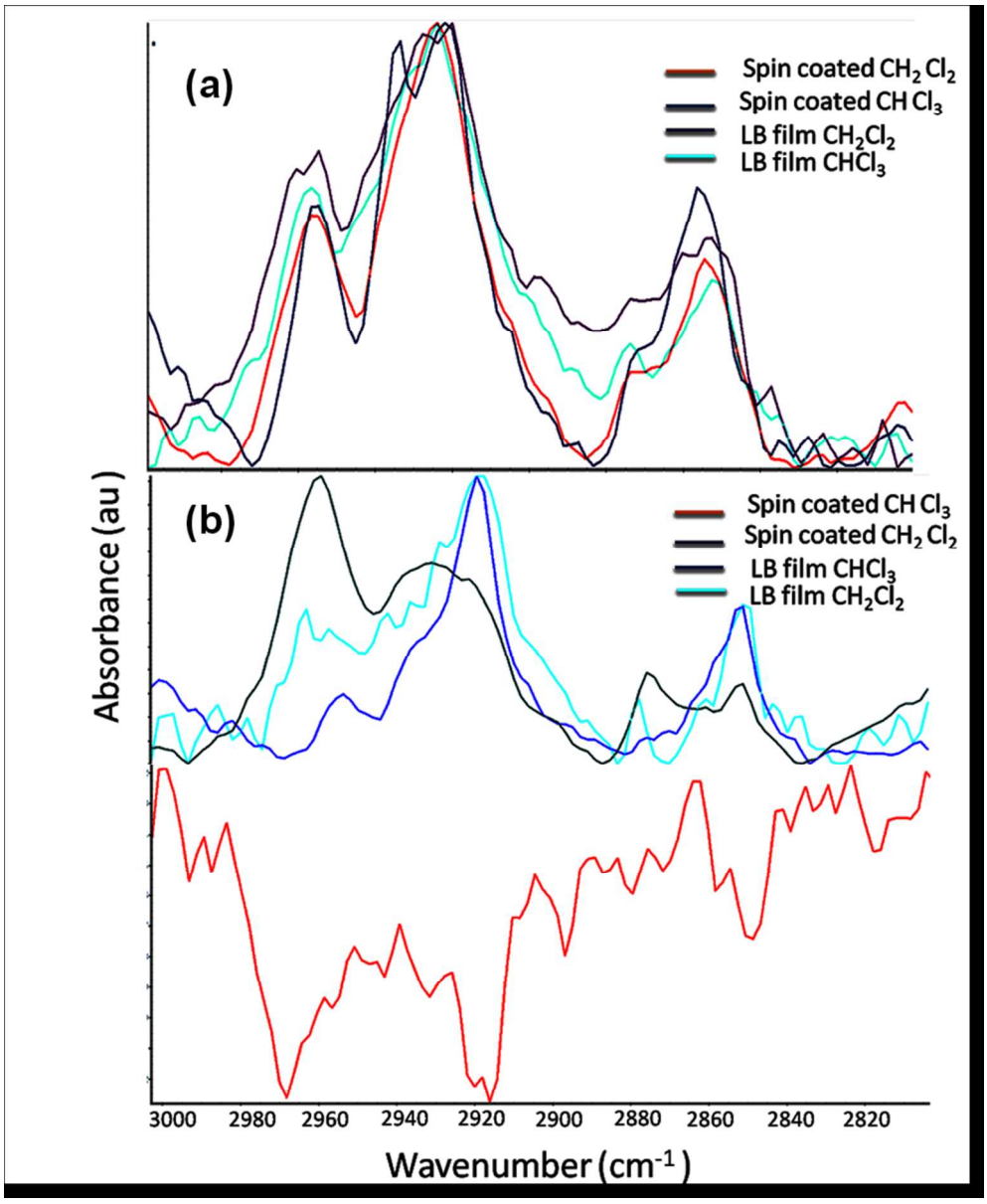

FT-IR overlaid spectrum of (a) PTC6 and (b) PTC14 samples in 2800-3000 cm-1 for LB and spin coated film prepared with two different (CH2Cl2/CHCl3) solvents
156x190mm (150 x 150 DPI)

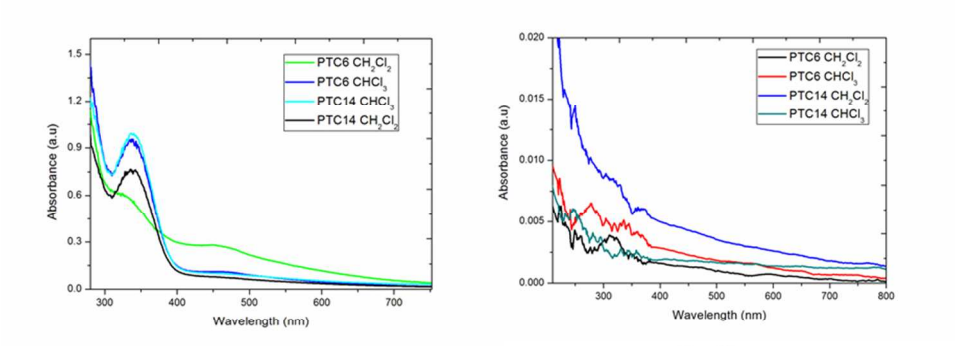

Fig.5a

Fig.5b

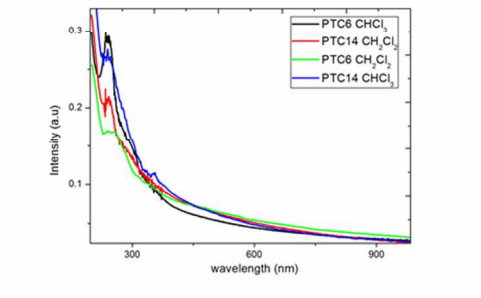

Fig. 5c

Absorption spectra of PTC6 and PTC14 (a) solution (b) LB film (C) spin coated film
254x190mm (96 x 96 DPI)

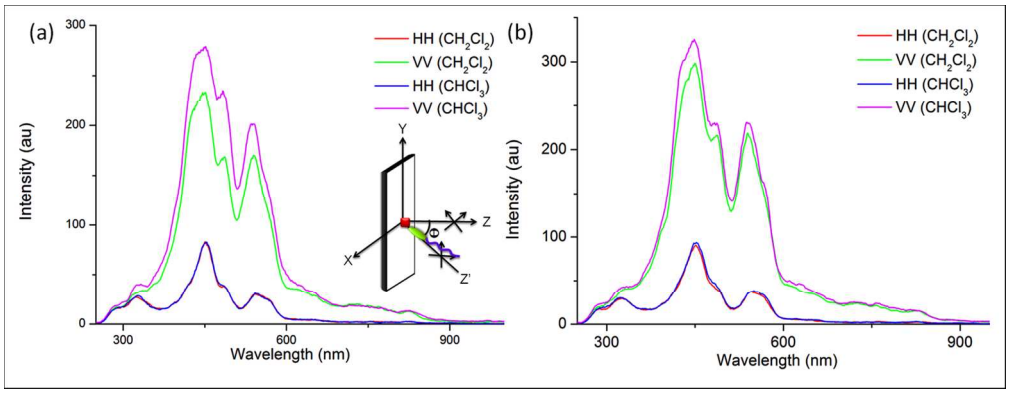

. Photo luminescence spectra of LB coated films of PTC6 (a) and PTC14 (b) in CHCl3 and CH2Cl2
272x104mm (150 x 150 DPI)

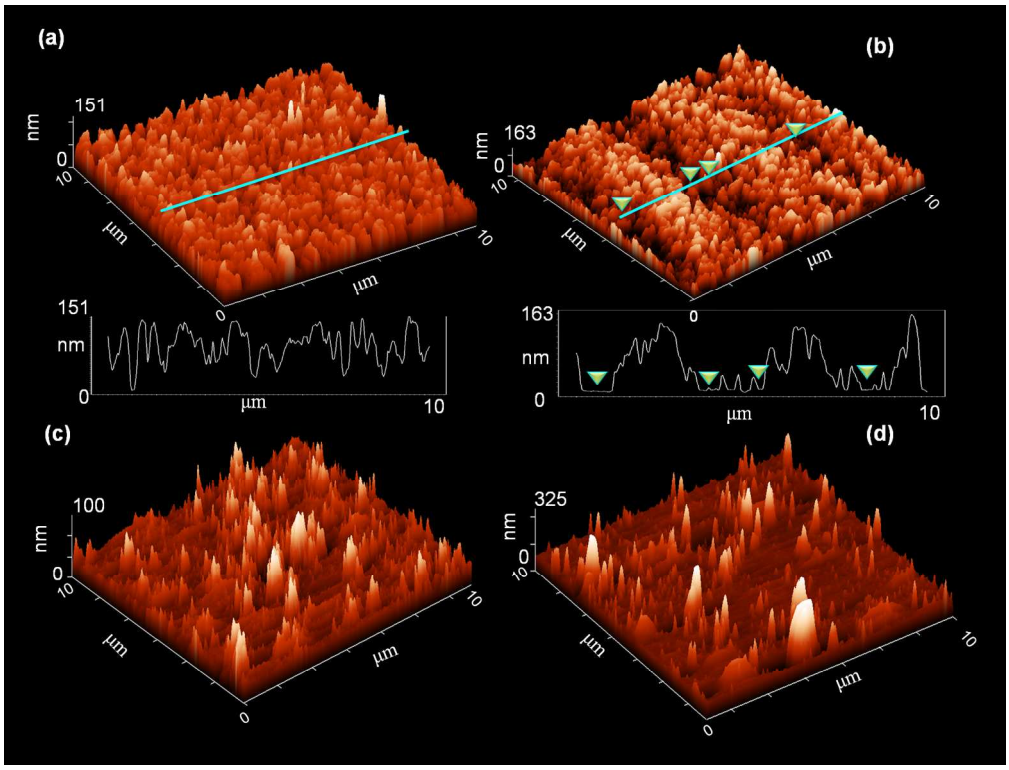

The AFM scanned image of PTC6 (a) CHCl3, (b) CH2Cl2; PTC14 (c) CHCl3, (d) CH2Cl2
323x245mm (150 x 150 DPI)

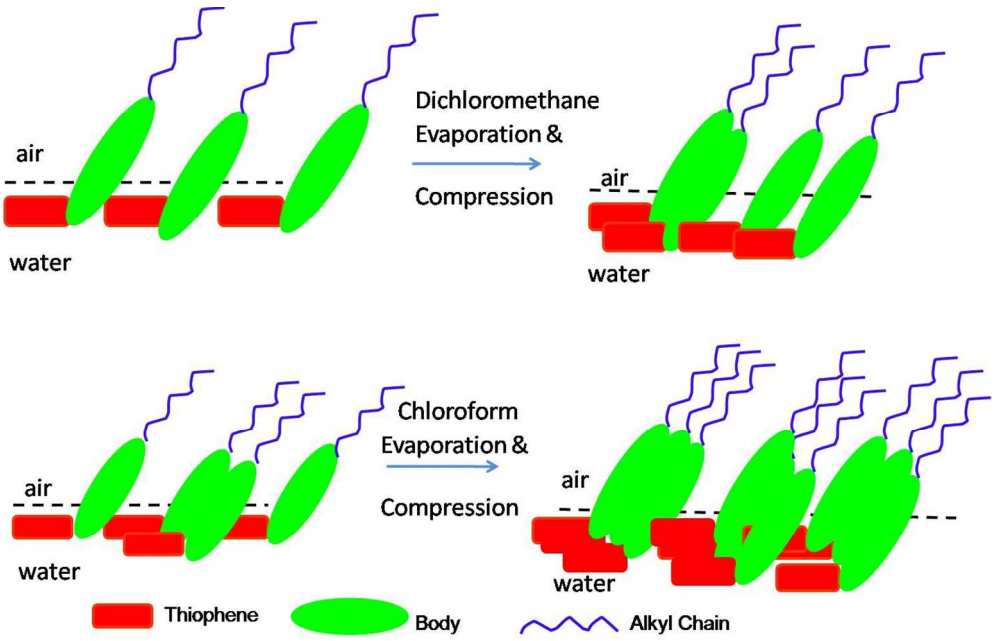

Schematic representation of dynamic bond variation organized according to the interaction between components with solvent and two different functionalities
245x154mm (150 x 150 DPI)